World Academy of Science, Engineering and Technology
International Journal of Aerospace and Mechanical Engineering
Vol:11, No:6, 2017

On the Free-Surface Generated by the Flow over an Obstacle in a Hydraulic Channel

M. Bouhadef, K. Bouzelha-Hammoum, T. Guendouzen-Dabouz, A. Younsi, T. Zitoun

Open Science Index, Aerospace and Mechanical Engineering Vol:11, No:6, 2017 publications.waset.org/10007750/pdf

***Abstract*—**The aim of this paper is to report the different experimental studies, conducted in the laboratory, dealing with the flow in the presence of an obstacle lying in a rectangular hydraulic channel. Both subcritical and supercritical regimes are considered. Generally, when considering the theoretical problem of the free-surface flow, in a fluid domain of finite depth, due to the presence of an obstacle, we suppose that the water is an inviscid fluid, which means that there is no sheared velocity profile, but constant upstream. In a hydraulic channel, it is impossible to satisfy this condition. Indeed, water is a viscous fluid and its velocity is null at the bottom. The two configurations are presented, i.e. a flow over an obstacle and a towed obstacle in a resting fluid.

***Keywords*—**Experiments, free-surface flow, hydraulic channel, subcritical regime, supercritical flow.

I. Introduction

WHEN a partially or completely immersed solid moves in a liquid, such as water, it undergoes a force which is a resistance to advance. This resistance is also called the hydrodynamic drag. The objective of the researchers working on hydrodynamics is, from immemorial time, to reduce this force so that the water slips better on the immersed bodies.

The problem of the flow above an uneven bottom is not in theoretically obvious. Indeed, the free-surface is unknown and analytical calculations, in particular for arbitrary forms of obstacles, are not easy. Thus, the analytical modeling of the free-surface is limited to thin obstacles, in linear theory. Besides the work of Lamb [1], we cite, without being exhaustive, Boutros et al., [2], Zitoun and Bouhadef [3] and Bouzelha et al. [4]. The first one shows that the analytical solution is expressed in series form. The subcritical free-surface aspect led to a local depression above the obstacle, followed by a downstream stationary wave train. Research of an adequate solution led many researchers to the development of various numerical processes such as Liapidevskii and Xu [5], Bouinoun et al. [6]. For the analysis of the resistance of vagueness, within the framework of the linear theory, Gadzar [7] used the method of the singularities; Euvrard [8] and Cherifi et al. [9] used the finite difference method. The finite element method was also used by Bai [10] and Forbes [11]. The results of the various studies showed that, contrary to the wavelength, the amplitudes are underestimated by the linear theory. The effect of the nonlinearities on the free-surface also was the subject of many works. It should however be noted that all the studies undertaken by Forbes and Schwartz [12], Cahouet and Lenoir [13], King and Bloor [14] and Bouhadef [15] are confronted with a problem of the choice of the adequate boundary condition making it possible to reveal the waves. Except for Bouhadef [15] and Amara and Bouhadef [16], the authors use the linear solution at a given stage of the calculation.

For the modeling of the supercritical flow (Fr> 1) above obstacle, in nonlinear theory, the most mainly adapted methods are the finite volume method and the finite element method. For this configuration, let us recall, among others, the work of King and Bloor [14], Ghaleb and Hefni [17], Bukreev [18], Bouhadef [15], Bouzelha-Hammoum et al. [19]. For example, Teniou [20] showed mathematically that the flow in presence of an obstacle lying on a flat bottom, in a hydraulic channel, generates necessarily a non-horizontal free-surface.

Unfortunately, few experimental works dealing with the free-surface flow in a hydraulic channel are available.

II. Mathematical Formulation

A. Governing Equations

Let us consider the two-dimensional free-surface flow of an inviscid incompressible fluid over an obstacle lying on the bottom of a hydraulic channel (Fig. 1). We note h the fluid depth far upstream where the flow is uniform with constant velocity U. We introduce the stream function ψ.

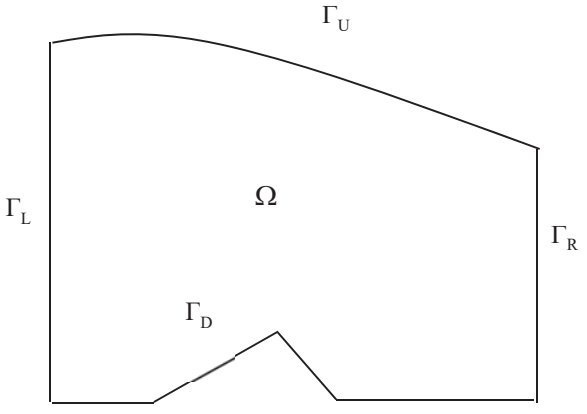

Fig. 1 Schematic geometry of the domain

M. Bouhadef, T. Guendouzen-Dabouz, A. Younsi and T. Zitoun are with the LEGHYD Laboratory, Faculty of Civil Engineering, University of Sciences and Technology HouariBoumediene (USTHB), BP 32, Bab-Ezzouar, Algiers, Algeria (e-mail: mbouhadef@usthb.dz).

K. Bouzelha-Hammoum is with the LEGHYD Laboratory, UMMTO, Algeria.

Open Science Index, Aerospace and Mechanical Engineering Vol:11, No:6, 2017 publications.waset.org/10007750/pdf

$F = U/\sqrt{gh}$ is the Froude number, Ω is the fluid domain, Γ_L, Γ_D and Γ_U the left, down and free-surface boundaries respectively.

Following Bouhadef et al. [21], the 2D problem, in dimensionless variables, is to find the stream function ψsatisfying the Laplace equation and the following boundary conditions, where y_0 is the free-surface position:

$$\Delta\psi = 0 \qquad \text{in } \Omega \qquad (1)$$

$$\psi = 0 \qquad \text{on } \Gamma_D \qquad (2)$$

$$\psi = y \qquad \text{on } \Gamma_L \qquad (3)$$

$$\partial\psi/\partial x = 0 \qquad \text{on } \Gamma_L \qquad (4)$$

$$\frac{\partial\psi}{\partial n} = \sqrt{1+\frac{2}{F^2}(1-y_0)} \qquad \text{on}\Gamma_U \qquad (5)$$

$$\psi = 1 \qquad \text{on } \Gamma_U \qquad (6)$$

On the downstream boundary Γ_R of the domain Ω, one should note that there is no natural boundary condition.

B. Mathematical Resolution

1. Finite Element Method Approach

To determine the unknown free-surface $y_0(x)$, we consider a sub-domain Ω' delimited by that free-surface, a part of the bottom Γ_D and the vertical columns I-1 and I+1.

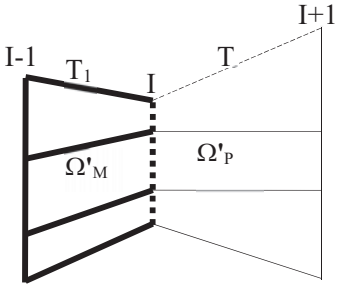

Fig. 2 Schematic computational domain

For each summit j of the column I (Fig. 2), we use the Green-Riemann identity to write:

$$\int_{\Omega'} \vec{\nabla}\psi.\vec{\nabla}\eta_{Ij}\, d\sigma = \int_{\Gamma'} \eta_{Ij}\frac{\partial\psi}{\partial n}\, ds = \int_{T_1\cup T} \eta_{Ij}\sqrt{C_1 - C_2\, y_0}\, ds$$

$$\int_{\Omega'} \vec{\nabla}\psi.\vec{\nabla}\eta_{Ij}\, d\sigma = \int_{T_1\cup T} \eta_{Ij}\sqrt{C_1 - C_2\, y_0}\, ds \qquad (7)$$

where $C_2 = 2/F^2$ and $C_1 = 1 + C_2$. y_0 is then determined by solving (7) which is written for j = n:

$$\int_{\Omega'} \vec{\nabla}\psi.\vec{\nabla}\eta_{In}\, d\sigma - \int_{T_1\cup T} \eta_{In}\sqrt{C_1 - C_2\, y_0}\, ds = 0 \qquad (8)$$

As explained in [16], this method allows to determine, step by step, the free-surface elevation. A highly nonlinear configurationis shown,for a sinusoidal obstacle (the ratiob/h is not small), in Fig. 3.

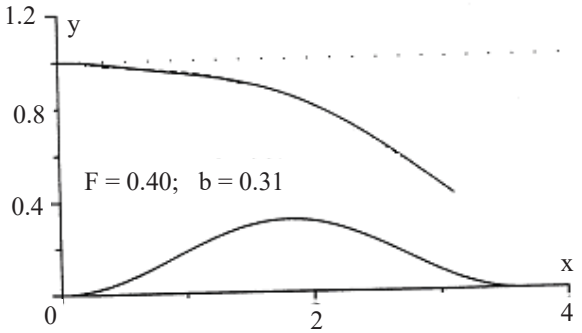

Fig. 3 Computed waveless free-surface

Numerical modeling of wavy free-surface flow for a subcritical regime is rather difficult because of, as already mentioned, the non-existence of an obvious boundary condition downstream of the obstacle. Several authors, such as Cahouet and Lenoir [13] use the boundary condition derived from the linear theory. The original method, based on the geometrical configuration described in Fig. 2, leads to a reasonable solution but, however, the wavelength is overestimated in relation to that which really exists.

In the case of a supercritical regime (F > 1), the downstream boundary condition is simpler to express, since the free-surface level tends to reach that of the undisturbed flow, andit can be expressed by:

$$\partial\psi/\partial x = 0 \qquad \text{on } \Gamma_R \qquad (9)$$

Recall that the iterative process consists on taking into account all the boundary conditions except the kinematic condition (6). This one is satisfied as [22]:

$$y(M') = \frac{1-\psi(M)}{\psi(N)-\psi(M)}\, y(N) + \frac{1-\psi(N)}{\psi(M)-\psi(N)}\, y(M)$$

where M is the point on the vertical located at the free-surface. N is the point situated just below M in the grid and M' the new point satisfying the condition $\Psi = 1$.

We give below the results obtained for a non-symmetrical obstacle and a highly non-linear configuration. The lower free-surface corresponds to the higher Froude number.

Open Science Index, Aerospace and Mechanical Engineering Vol:11, No:6, 2017 publications.waset.org/10007750/pdf

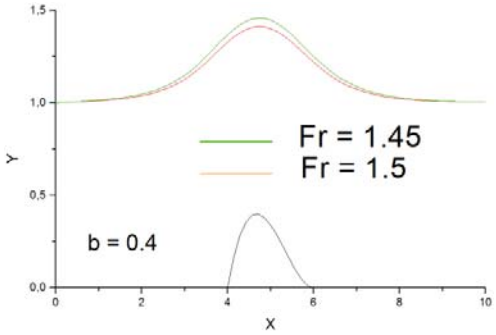

Fig. 4 Computed free-surface (F>1)

2. Finite Volume Method Approach

When using the finite volume method, the formulation is put in the form:

$$\varepsilon \frac{\partial \psi}{\partial t} + \overline{\text{div}\,[\vec{F}\,(\psi)]} = S_\psi \qquad (10)$$

$\varepsilon = 1$ for unsteady problems, $\vec{F}\,(\psi)$ is the total flux vector, S_ψ is a source term. For our steady problem, (10) is simplified because of the absence of a source term:

$$\text{div}\,[\vec{F}\,(\psi)] = 0 \qquad (11)$$

The function ψ being harmonic ($\Delta\psi = 0$), the vector $\vec{F}$ is thus related to ψ by:

$$\vec{F} = \overrightarrow{\text{grad}}\,\psi \qquad (12)$$

For a domain Ω_K of boundary occupied by the cell K, and using the Green's theorem, (10) can be written:

$$\int_{\Gamma_K} \vec{F}.\vec{n}\, ds = 0 \qquad (13)$$

Let us consider a cell K(i,j) which has two borders (i-1), (i+1) along **x** and two others (j-1)), (j+1) along **y**. The boundary Γ_K in (13) is then the union of these four boundaries and the vector $\vec{F}$ is related to ψ by (12), at the centre of the cell.

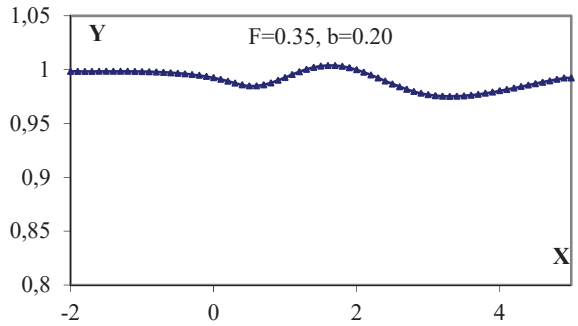

Fig. 5 Computed free-surface (F<1, Lmax=5)

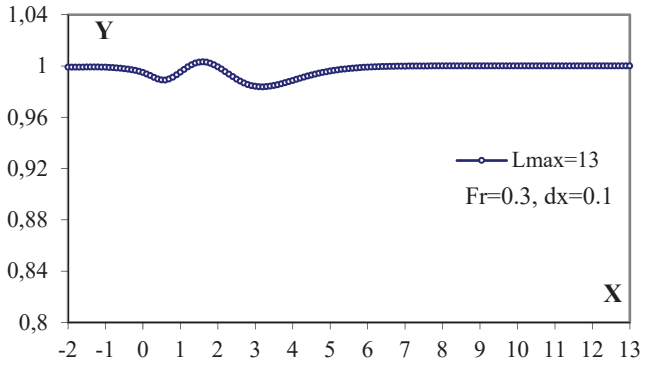

Fig. 6 Computed free-surface (F<1, Lmax=13)

For a wavy subcritical regime, the numerical process leads, of course, to waves but they are located only above the obstacle, as shown in Fig. 5.

When the computational domain is long enough (Fig. 6), the level of the free surface joins that of the upstream.

As already mentioned by Euvrard [8], the boundary conditions upstream and downstream are almost identical, giving rise to a mainly similar free-surface far upstream and far downstream. To create the waves, one must take into account the physical phenomenon. It is known that, contrary to capillary waves, the group velocity of gravity waves is positive, which implies that the direction of propagation must appear under the boundary conditions. These are too symmetrical, which results in a similar behavior of the free-surface upstream and downstream. Cherifietal. [9] use the velocity potential formulation for the resolution of the problem. The undulated free-surface obtained is symmetrical. The physical phenomenon usually observed is devoid of waves upstream for a subcritical regime at low Froude numbers; they exist only downstream. In the digital process, the waves should be damped only upstream. Such as Euvrard [8], an artificial viscosity is introduced, but only upstream. Namely, one replaces the free-surface boundary condition

$$\frac{g}{U^2}\phi_y + \phi_{xx} = 0 \qquad (14)$$

by:

$$\frac{g}{U^2}\phi_y + \phi_{xx} + \varepsilon\,\phi_{xxx} = 0 \qquad (15)$$

where g is the acceleration due to gravity and U the uniform upstream velocity.

The obtained free-surface, for two values of the artificial viscosity ε, is given below (Fig. 7).

Amara and Bouhadef [16], using a finite element method, with a Neumann boundary condition far downstream, obtain the shape shown on Fig. 7, which is an almost symmetrical waveless free-surface, between the upstream and the downstream side.

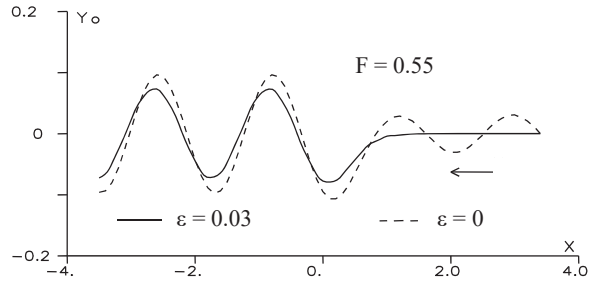

Fig. 7 The influence of the artificial viscosity ε

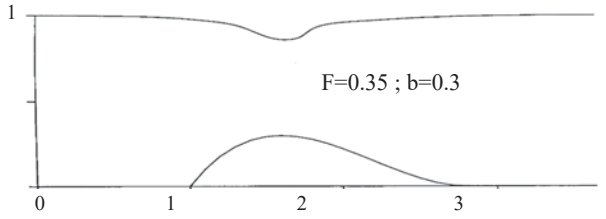

Fig. 8 Aspect of the computed free-surface

3. Analytical Approach

Let us consider the free-surface generated by two or many coupled obstacles lying on the bottom and pulled at a velocity U in a hydraulic channel where the water is otherwise at rest (Fig. 7). To easily carry out analytical formulation, in linear theory, the obstacle shape is chosen triangular. The function f(x) describing it is thus given by:

$$f(x) = \begin{cases} 0 & \text{for } x \le 0 \\ x\ tg\gamma & \text{for } 0 \le x \le L/2 \\ -x\ tg\gamma + 2b & \text{for } L/2 \le x \le L \\ 0 & \text{for } x \ge L \end{cases}$$

with $tg\gamma = \frac{2b}{L}$, where b and L are respectively the height and the length of the obstacle.

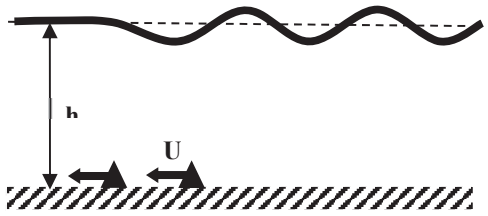

Fig. 9 Physical formulation

Using the Lamb's method, Ouatiki et al. [23] give the equation of the free-surface elevation $y_0(x)$:

$$y_0 = \frac{b}{L(F^2-1)}\left(|x| - \left|x - \frac{L}{2}\right|\right) - \frac{2F^2 b}{L}\sum_{n=Fr^2\cos^2\beta_n - 1}^{n=} \frac{\cos\beta_n}{\cos^2\beta_n - 1}\left(e^{-y_n\left|x-\frac{L}{2}\right|} - e^{-y_n|x|}\right) +$$
$$\frac{b}{L(F^2-1)}\left(|x-L| - \left|x - \frac{L}{2}\right|\right) - \frac{2F^2 b}{L}\sum_{n=F^2\cos^2\beta_n - 1}^{n=} \frac{\cos\beta_n}{\cos^2\beta_n - 1}\left(e^{-y_n\left|x-\frac{L}{2}\right|} - e^{-y_n|x-L|}\right) +$$
$$\frac{2F^2\, b\, ch\,\alpha}{L\alpha(F^2\, ch^2\alpha - 1)}\left[\sin\alpha\, x + \sin\alpha\left|x\right| - \sin\alpha\left(x - \frac{L}{2}\right) - \sin\alpha\left|x - \frac{L}{2}\right|\right] +$$
$$\frac{2F^2\, b\, ch\,\alpha}{L\alpha(F^2\, ch^2\alpha - 1)}\left[\sin\alpha(x - L) + \sin\alpha\left|x - L\right| - \sin\alpha\left(x - \frac{L}{2}\right) - \sin\alpha\left|x - \frac{L}{2}\right|\right]$$

where F is the Froude number.αandβ_n are respectively the solutions of the equations $\tanh\alpha = F^2\alpha$ and $\tan\beta_n = F^2\beta_n$.If d is the distance which separates two identical triangles, the free-surface wave amplitude is given by:

$$A = \frac{8F^2\, b\, ch\,\alpha}{F^2 ch2\alpha - 1}\,\frac{\sin 2\alpha\frac{L}{4}}{\alpha\frac{L}{4}}\cos\alpha\frac{d}{2}\left[\sin\alpha\left(x - \frac{L+d}{2}\right)\right]$$

The distance between the obstacles can thus substantially modulate,for a given obstacle length, the free-surface wave amplitude.

4. Gravity-Capillarity Waves

Let us first recall that in the theoretical studies mentioned above, the fluid is assumed inviscid and the capillarity is not taken into account. Otherwise, the Navier-Stokes equations must be used with the appropriate boundary conditions, such as the no slip condition, the cinematic condition and the existence of the surface tension at the free-surface.

Following Bouhadef [24], Younsi et al. [25], the governing differential equation of the pressure P and the boundary conditions associated can be written, in dimensionless variables, as:

$$P'' - \frac{2F}{FU-\beta}P'U' - \varepsilon^2 P = 0 \quad (5.1)$$

$$P'(0) = 0 \quad (5.2)$$

$$P'(1) = \frac{\varepsilon^2\left[\beta - FU(1)\right]^2}{1 + B\varepsilon^2}P(1)$$

whereβ is the phase velocity, B is the Bound number, U(y) is the dimensionless velocity profile, U' its first derivative. The determination of the dimensionless wave number $\varepsilon = 2\pi\frac{h}{\lambda}$ (h is the mean water depth) leads tothe resolution of an eigenvalues problem.

The addition of a condition related to the amplitude of the wave and the disturbance discharge,such as in Bouhadef [24], allows the pressure calculation.

$$P(1) = \frac{1 + \varepsilon^2 B}{\beta - F\,U(1)}$$

Open Science Index, Aerospace and Mechanical Engineering Vol:11, No:6, 2017 publications.waset.org/10007750/pdf

Open Science Index, Aerospace and Mechanical Engineering Vol:11, No:6, 2017 publications.waset.org/10007750/pdf

The main results that the authors have shown can be summarized, according to the Fig. 10, by:

– the velocity profile shape plays a non-negligible role in the variation of the standing waves of gravity and capillarity.
– the free surface velocity mainly determines the wavelength of the capillary waves.

III. Experimental Study

A. Apparatus

The basic device is a hydraulic channel, with variable slope, consisting of juxtaposed glazed elements over a length of ten meters, of uniform rectangular cross-section. This channel was arranged so as to retain a quantity of water at rest at a given height. A system consisting of pulleys, a drum, and wire, is positioned in the channel so as to move an obstacle in otherwise resting water. The free-surface is then the seat of standing gravity waves (Fig. 11).

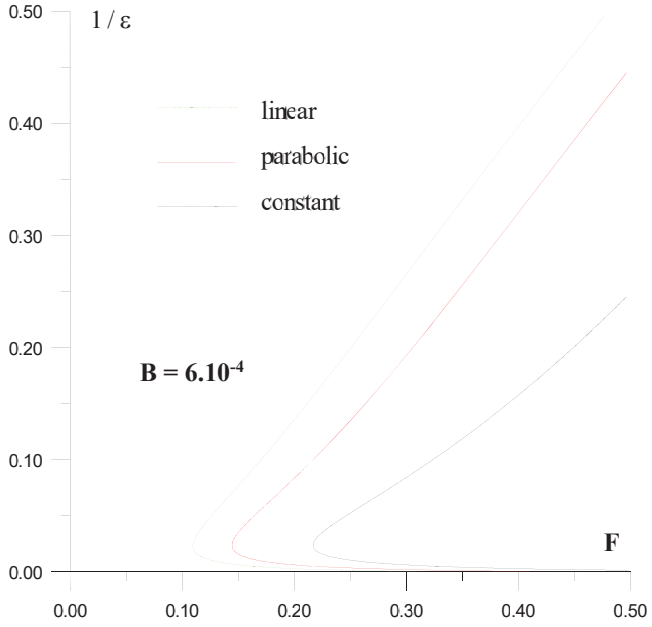

Fig. 10 Wavelength versus Froude number

Fig. 11 Free-surface standing gravity waves

As soon as the carriage moves, the rod flushing the surface of the water generates capillary waves upstream of that rod (Fig. 12).

For the supercritical regime, the experimental study was carried out in a Plexiglas hydraulic channel of uniform rectangular cross-section of width b = 7.5 cm and length 6 m. The channel is fed in a closed circuit by a pump. In order to obtain high velocity flows, a convergent (Fig. 12) has been added at the entrance to the channel.

Thus, by choosing a suitable height H at the output of the nozzle, we can reach values of the Froude number F that are clearly greater than 1, for different flow rates Q. The flowmeter is previously calibrated and the relationship between the real flow rate and the indicated one is given by:

$Q = 1.0522Q_r - 0.0001$ where Q_r (m^3/s) corresponds to the value read and Q the effective discharge.

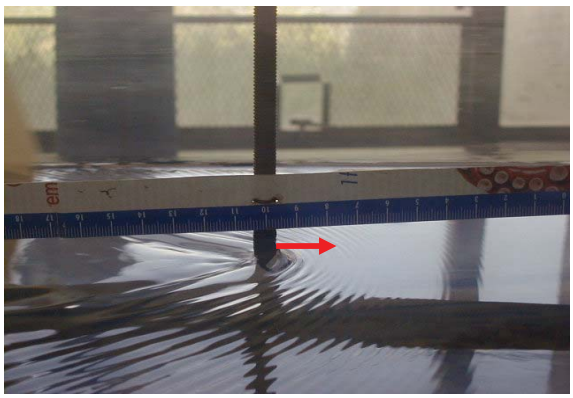

Fig. 12 Standing capillary waves

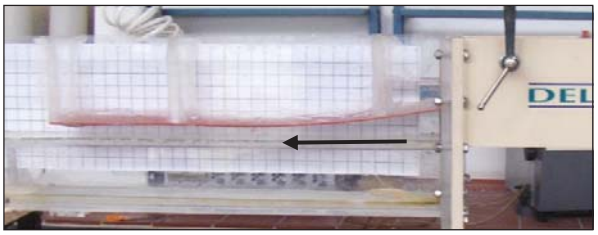

Fig. 13 Nozzle upstream for a supercritical regime

B. Results

1. Supercritical Regime

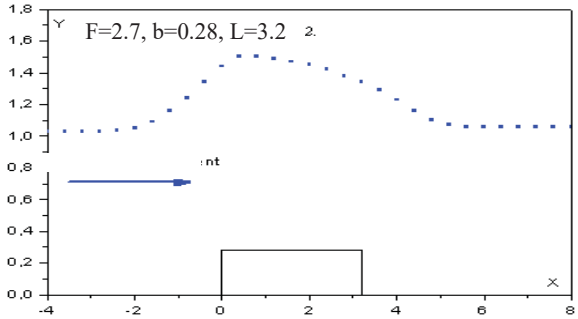

Fig. 14 Supercritical regime over a step

If b is the dimensionless height of the obstacle lying on the bottom of the channel, relatively to the water depth, the asymmetrical free-surface measured, by way of example, has the shape given above. Recall that, as we had previously

Open Science Index, Aerospace and Mechanical Engineering Vol:11, No:6, 2017 publications.waset.org/10007750/pdf

mentioned it, in the theoretical part dealing with the boundary conditions, the free-surface, in the supercritical configuration, is practically horizontal far upstream and downstream of the obstacle (Fig. 13).

2. Subcritical Regime

As it is shown below, the free-surface may be the seat of standing waves.

If two obstacles move at the bottom of a hydraulic channel at a moderate velocity, the free-surface (Fig. 15) depends not only on the Froude number calculated with that traction speed, but also on the distance **d** between the obstacles.

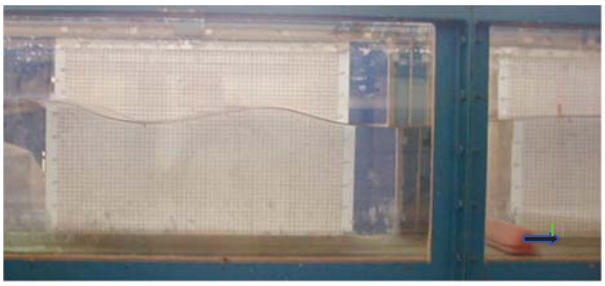

Fig. 15 Standing free-surface waves

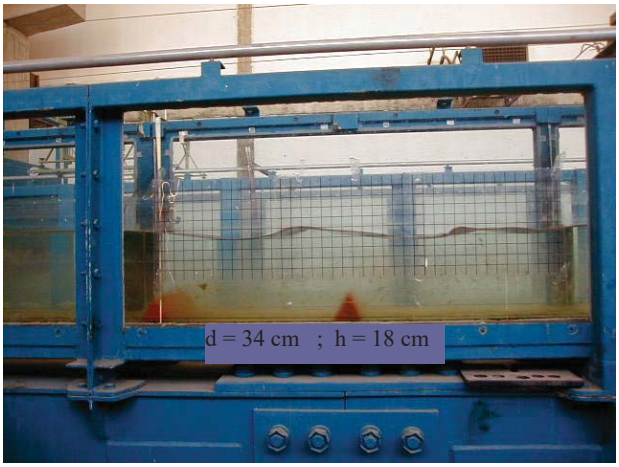

Fig. 16 Free-surface waves over two obstacles

3. Capillarity Waves

Depending on the Froude number value, the dimensionless wavelength of the standing free-surface waves varies. On the Fig. 16, we represent the obtained experimental results for the capillary waves with the same water depth h_0 = 18 cm, compared to those given by the numerical method. Even for the standing gravity waves, the agreement is reasonably good, as already mentioned by Younsi et al. [25] and shown on the Fig. 17.

IV. Conclusion

As it was already mentioned, in Bougamouza et al. [26], for example, one shows, through the experimental study carried out in a hydraulic channel, that one can establish the supercritical mode by only adding a convergent at the entry of the channel.

In order to satisfy, as much as possible, the boundary conditions due to the assumed inviscid fluid hypothesis, one must consider experimentally the flow generated by the movement of an obstacle in a fluid otherwise at rest. Indeed, in the case of the flow of a fluid above a submerged obstacle, the velocity profile is necessarily sheared and cannot be uniform upstream.

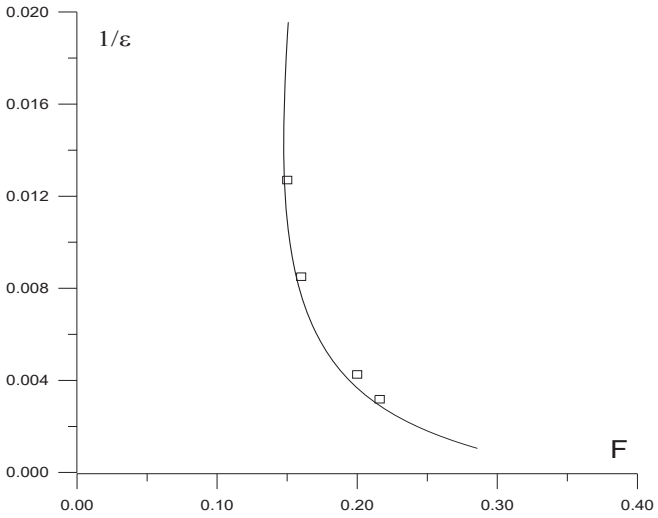

Fig. 17 Capillary wavelength versus Froude number

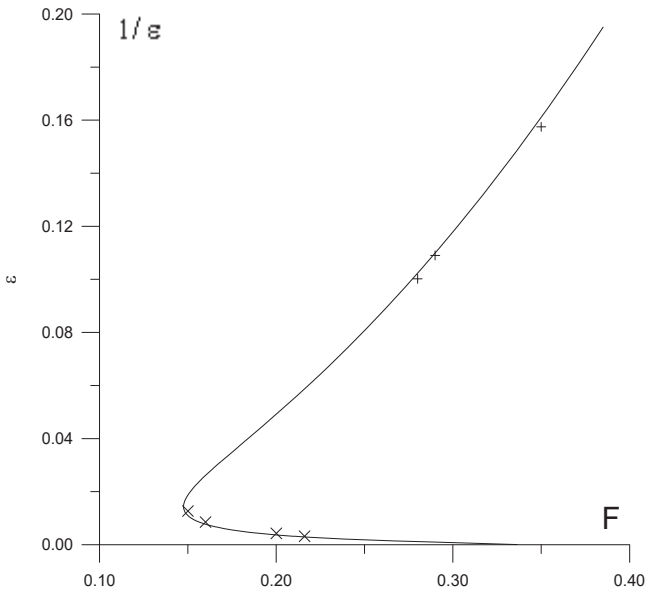

Fig. 18 Theoretical and experimental wavelength evolution

Acknowledgment

The authors would like to thank the DGRSDT (Algeria) for its financial support to the LEGHYD laboratory.

References

[1] Lamb H., 1945, Hydrodynamics, 6th ed. Dover, New York
[2] Boutros Y.Z., Abdelmalek M.B. and MassoudS.Z., 1986, Linearized solution of a flow over a non-uniform bottom, J. of Comput and Appli. Math., 16, 105-116

Open Science Index, Aerospace and Mechanical Engineering Vol:11, No:6, 2017 publications.waset.org/10007750/pdf

[3] Zitoun T. andBouhadef M.,1993, Solution linéaire analytique de l'écoulement à surface libre au-dessus d'un fond perturbé, 1er Congrès de Mécanique, Rabat
[4] Bouzelha K., Cherifi F., Bouhadef M.,1997, Etude des écoulements à surface libre au-dessus d'un fond non uniforme, 2ème Colloque Maghrébin sur l'Hydraulique, Zéralda, Alger
[5] Liapidevskii V. Y. and Xu Z., 2006, Breaking of waves of limiting amplitude over an obstacle, Journal of Applied Mechanics and Technical Physics, Vol. 47, No. 3, pp. 307–313
[6] Bouinoun M., Bouhadef M. and Zitoun T., 2012,Free surface flowoveran uneven bottom:Experiments in ahydraulic channel,International Conference on Metallurgical, Manufacturing and Mechanical Engineering, Dubai, UAE
[7] Gazdar A.S.,1973, Generation of waves of small amplitude by an obstacle placed on the bottom of a running stream,J. Phys. Soc. Japan 34, 2
[8] Euvrard D.,1976, Sur la possibilité d'une résolution numérique directe du problème de Neumann Kelvin, par introduction d'une perturbation singulière, C. R. Acad. Sc. Paris, 262, A
[9] Cherifi F., Bouhadef M., Bouzelha K., Zitoun T. and Benabdellah C., 2006, Numerical resolution of a linear free surface waves problem with an artificial viscosity,CHISA'2006, Praha
[10] Bai K.J., 1977, A localized finite element method for steady two-dimensional free surface flow problems, 1st. Int. Conf. on Numer. Ship Hydrodyn. Gaithersburg, Maryland, 209
[11] Forbes L. K., 1981, On the wave resistance of a submerged semi-elliptical body, J. of Engeneer. Math. 15, 287
[12] Forbes L. K., Schwartz L. W., 1982, Free-surface flow over a semicircular obstruction, J.Fluid Mech., 114, 299, 314
[13] Cahouet J., Lenoir M., 1983, Résolution numérique du problème non linéaire de la résistance de vagues bidimensionnelle, C.R.Acad. Sci. de Paris. 297
[14] King A.C., Bloor M.T.G., 1987, A free surface flow over a step, J. Fluid. Mech. 182, 193-208
[15] Bouhadef M., 1988, Contribution à l'étude des ondes de surface dans un canal hydraulique. Application à l'écoulement au-dessus d'un obstacle immergé, Thèse de Doctorat-ès-Sciences, U.E.R. C. E. A. T., Poitiers (France)
[16] Amara M, Bouhadef M.,1991, A new approach of numerical modelling of 2D surface waves induced by an obstacle, Computer Meth. and Water Ress. C. M. P.
[17] Ghaleb A.F., Hefni A.Z., 1987, Wave free, two-dimensional gravity flow of an inviscid fluid over a bump, J. Mec. Theor. Appl., 6, 4
[18] Bukreev V. I., 2002, Supercritical flow over a sill in an open channel, Journal of Applied Mechanics and Technical Physics, Vol. 43, No. 6
[19] Bouzelha-Hammoum K., Bouhadef M., Zitoun T.and Guendouzen T., 2008, Contribution to the study of a free-surface supercritical flow above an obstacle: theory and laboratory work, 6th IASME/WSEAS International Conference on Fluid Mechanics and Aerodynamics
[20] Teniou D., 2007, Sur l'écoulement d'un fluide dans un canal avec obstacle au fond, Annales mathématiques Blaise Pascal, Vol. 14, n°2
[21] Bouhadef M., Zitoun T., Guendouzen T., 2004, Contribution to numerical and experimental study of 2D free-surface flow, IASME Transactions Journal, Issue 3, Vol. 1
[22] Bouzelha-Hammoum K., Bouhadef M., Zitoun T., 2006, Numerical study of 2D free-surface waveless flow over a bump, WSEAS Transactions on Fluid Mechanics, Issue 6, Vol. 1, 732-737
[23] Ouatiki K., Younsi A., Bouhadef M., Zitoun T., Guendouzen T, 2004, Free surface waves induced by two or many coupled obstacles, CHISA'2004, Praha
[24] Bouhadef M.,1993, The influence of a sheared velocity profile on the wavelength of standing small amplitude surface waves, Computer Methods and Experimental Measurements VI, Vol. 1, Computational Mechanics Publications
[25] Younsi A., Bouhadef M, Guendouzen-Dabouz T.,2007, Contribution to the numerical and experimental study of gravity capillary waves in a hydraulic channel: the influence of a sheared velocity profile, International Conference on Fluid Mechanics and Aerodynamics, Vouliagmeni, Athens
[26] Bougamouza A, Guendouzen-Dabouz T., Bouzelha-Hammoum K., Bouhadef M.andZitoun T., 2010, 2D supercritical free-surface flow: an experimental study, HEFAT 2010, Antalya.